*Combust. Sci. and Tech.*, 1998, Vol. 134, pp. 291–314
Reprints available directly from the publisher
Photocopying permitted by license only



# Partitioning of the Refractory Metals, Nickel and Chromium, in Combustion Systems

W. P. LINAK[a,*] and J. O. L. WENDT[b]

[a] *Air Pollution Prevention and Control Division, MD-65*
*National Risk Management Research Laboratory,*
*U.S. Environmental Protection Agency, Research Triangle Park, NC 27711 USA;*
[b] *Department of Chemical and Environmental Engineering,*
*University of Arizona, Tucson, AZ 85721 USA*

*(Received 2 March 1998)*

The partitioning of nickel (Ni) and chromium (Cr) in a laboratory scale combustor was investigated theoretically and experimentally. Theoretical predictions based on chemical equilibrium indicate that chlorine significantly increases the volatility of Ni because of the formations of Ni-chloride compounds. Chlorine's predicted effect on Cr volatility at high temperatures (> 700 K) was minimal, although some volatile Cr-chloride compounds were predicted at low temperatures (< 700 K).

Experimental studies employed a 59 kW laboratory scale combustor with a swirling natural gas diffusion flame through which aqueous Ni and Cr solutions were sprayed. Particle size distributions (PSDs) in the stack were measured by three different techniques: electrical mobility and inertial impaction for sampled aerosols and light scattering for *in-situ* analyses. All three methods produced consistent PSDs. Experimental data for Ni were also consistent with the theoretical predictions, and confirmed the large increase in Ni volatility due to chlorine. Also consistent with equilibria, experimental data for Cr(III, VI) failed to indicate notable increases in volatility due to chlorine addition. However, introducing Cr(VI) in the feed produced smaller Cr particles in the exhaust than did Cr(III). Experimental evidence suggests that, contrary to equilibrium predictions, Cr(VI) vaporized in the flame while Cr(III) did not. This result, however, may not be related to the initial Cr valency but, rather, due to the particular choice of Cr(III) [$Cr(NO_3)_3$] and Cr(VI) [$CrO_3$] species examined. Speciation of Cr in the exhaust, however, was independent of the initial Cr valency, with exhaust values of Cr(VI) typically less than 1% of the total Cr measured. Based on color and solubility, a large fraction of the sampled Cr was believed to be $Cr_2O_3$. The Cr(VI) fraction in the exhaust was enhanced slightly by chlorine, but reduced to below analytical detection limits by the addition of small (stoichiometric with respect to Cr) quantities of sulfur.

* Corresponding author. E-mail: blinak@inferno.rtpnc.epa.gov

Once vaporized with chlorine, Ni was readily scavenged by kaolinite. However, kaolinite had no effect on the PSD of non-volatile Ni (without chlorine), and both kaolinite and hydrated lime had no effect on the PSDs for Cr(III, VI), whether it vaporized or not (with and without chlorine).

*Keywords:* Waste incineration; chromium speciation; hexavalent chromium; metal transformations; transition metals; particle formation

## INTRODUCTION

Toxic elements are present in the effluents of many combustion processes, including coal and oil fired utilities, industrial operations, and thermal processes for the treatment of municipal and hazardous wastes (Linak and Wendt, 1993). Fourteen metals, including the metalloids antimony and arsenic, and the element selenium are currently regulated in the U.S. under the Clean Air Act Amendments (CAAA, 1990) and the Resource Conservation and Recovery Act (RCRA, 1986; Fed. Reg., 1991; Garg, 1992). While antimony, arsenic, and selenium typically exhibit only weak metallic properties, they are defined here as metals for simplicity. Trace elements are often classified based on their behavior in combustion systems, and this behavior can be related to their relative volatilities. In a review of the coal combustion and gasification literature, Clarke and Sloss (1992) identify three overlapping groups. Group 3 elements volatilize most readily and are concentrated in the gas phase and depleted in all solid phases. Group 2 elements are enriched on the fine-grained particles which may escape particulate control systems. Group 1 elements are concentrated in the coarse residues or are partitioned equally between these residues and fly ash particulates. These elements are generally trapped by particulate control systems. Rizeq *et al.* (1994) also group these metals into three volatility classes which correlate approximately with the groups identified above. Mercury and selenium, tend to be volatile, even at moderate stack temperatures. Antimony, arsenic, cadmium, lead, and thallium, are of medium volatility (semi-volatile), and have the potential of vaporizing at the high temperatures in the flame zone. Finally, a third group including barium, beryllium, chromium (Cr), and nickel (Ni), are considered to be non-volatile (refractory) over the entire range of typical combustion temperatures encountered. The metals cobalt and manganese are not classified by Rizeq *et al.* (1994), but are classified as Group 1 elements by Clarke and Sloss (1992). The final regulated metal, silver, is not classified by either study, but based on the volatility of several species expected to be formed within combustion environments, silver would also likely

be classified as non-volatile. Whereas most attention, heretofore, has been focused on the behavior and partitioning of the volatile and semi-volatile metals, this paper focuses on Ni and Cr which are generally considered to be refractory.

Volatile and semi-volatile metals have been of interest because they remain as vapors within combustion and flue gas cleaning systems resulting in poor removal efficiencies, or tend to form fumes of submicron particles resulting from nucleation and condensation of metal vapor. These mechanisms lead to substantial enrichment of toxic metals on submicron particles which are often difficult to collect in particulate pollution control equipment. Scotto *et al.* (1992); Wendt (1994) and Linak *et al.* (1995) demonstrated that some metal vapors react at high temperatures (above their dewpoints) with sorbents to form environmentally benign water insoluble products. Thus, the emissions of some of these volatile and semi-volatile metals can be managed. Several researchers (Davison, 1974; Klein *et al.*, 1975; Markowski *et al.*, 1980 and Quann and Sarofim, 1982) have also noted enrichment of the refractory metals Ni and Cr in submicron particles, even though it is not obvious that these metals necessarily vaporize in the combustion process. The mechanisms by which this occurs are not readily apparent. It is appropriate, therefore, to focus on refractory metals, and to determine if their partitioning among various particle sizes can be predicted and controlled.

Ni is slightly less volatile than Cr (boiling points of 3003 K and 2945 K, respectively). Cr exists in two forms in the environment (Goyer, 1991; Seigneur and Constantinou, 1995), as either trivalent Cr(III) or hexavalent Cr(VI), as in the chromate anion $CrO_4^{2-}$ or in the compound $CrO_3$. Cr(VI) has the lowest risk specific dose for all carcinogenic metals (0.00083 $\mu g/m^3$) (Fed. Reg., 1991), while Cr(III) is not considered particularly hazardous. However, from a regulatory viewpoint, all Cr must be considered to be Cr(VI) unless difficult site specific speciation is performed.

Linak *et al.* (1996) determined that regardless of the initial valency of Cr, only a small fraction of the total Cr in the exhaust of a research combustor occurs as Cr(VI). We focus here not only on how Cr is chemically partitioned between valency states in the exhaust, but also on how this can be manipulated through the addition of other compounds, such as sulfur and chlorine, and how the physical partitioning of Cr among various particle sizes occurs in a practical combustion configuration. While the previously published research focused on Cr speciation and factors which influence the chemical partitioning of Cr(VI) and total Cr, this research emphasizes factors which influence particle formation and the resultant metal particle

size distributions (PSDs). To accomplish this, three particle sizing methods are used: inertial impaction, electrical mobility, and *in-situ* light scattering. Additional morphological information is provided by field emission scanning electron microscopy. Throughout this paper, recent Cr data are compared to Ni data taken in the past (Linak *et al.*, 1994, 1995). This is done to correlate similarities and contrast differences between two seemingly similar refractory metals.

## THEORY: EQUILIBRIUM CONSIDERATIONS

Multicomponent equilibrium calculations can provide insight into which species are thermodynamically stable at flame and flue gas temperatures. Previous literature on equilibrium predictions exist in the work of Wu and Biswas (1993); Frandsen *et al.* (1994) and Owens *et al.* (1995). As always, the accuracy of equilibrium results depends on the accuracy of the thermodynamic data available, and on the availability of thermodynamic data for all important species containing the elements in question. In addition, equilibrium calculations do not take into account kinetic or mixing limitations and represent, therefore, an idealized solution that may not be realized in practical systems. Thermochemical predictions were determined using the CET89 computer code for calculating complex chemical equilibrium compositions (Gordon and McBride, 1986). Table I lists the metal species considered in these calculations, together with the appropriate references. Note that the chlorinated Cr species list has been updated and differs from that used by Wu and Biswas (1993) and by Linak and Wendt (1993), and so new and different equilibrium results might be expected. Of interest is the thermodynamic partitioning between vapor and condensed phases, as well as the partitioning between various species. Also, of special interest for Cr is the partitioning between Cr(VI) and Cr(III) species (see Linak *et al.*, 1996). Conditions, summarized in Table II, represent combustion of natural gas at a stoichiometric ratio of 1.2, with aqueous metal solutions injected to produce nominally 100 ppm metal in the exhaust. Effects of chlorine (0–2900 ppm chlorine) and sulfur (0–2800 ppm sulfur) were investigated.

Equilibrium predictions (Fig. 1a), which complement the prior Cr species predictions of Linak *et al.* (1996), indicate that both metals are refractory, with dewpoints of 2000 K and 1900 K for 100 ppm Ni and Cr, respectively. Chlorine addition (Fig. 1b) lowers the Ni dewpoint by approximately 100 K, but has no significant effect on Cr. The fact that chlorine is more likely to vaporize Ni than Cr at high temperatures, suggests that, in the presence of

TABLE 1 Nickel and chromium species considered for equilibrium calculations

| *Species without chlorine or sulfur* | | *Additional species with chlorine* | | *Additional species with sulfur* | |
|---|---|---|---|---|---|
| *Ni species* | *Reference* | *Ni species* | *Reference* | *Ni species* | *Reference* |
| Ni | J12/76 | NiCl | J9/77 | NiS | J12/76 |
| NiO | L2/84 | $NiCl_2$ | IB93 | NiS(*a*) | J12/76 |
| $Ni(CO)_4$ | IB89 | $NiCl_2(s)$ | IB93 | NiS(*b*) | J12/76 |
| $NiO_2H_2$ | L3/84 | $NiCl_2(l)$ | IB93 | NiS(*l*) | J12/76 |
| Ni(*s*) | J12/76 | | | $NiS_2(s)$ | J3/77 |
| Ni(*l*) | J12/76 | | | $NiS_2(l)$ | J3/77 |
| $Ni_3C(s)$ | B5/89 | | | $Ni_3S_2$(I) | J12/76 |
| $NiCO_3(s)$ | B5/89 | | | $Ni_3S_2$(II) | J12/76 |
| NiO(1) | BAR73 | | | $Ni_3S_2(l)$ | J12/76 |
| NiO(2) | BAR73 | | | $Ni_3S_4(s)$ | J3/77 |
| NiO(3) | BAR73 | | | $NiSO_4(s)$ | IB93 |
| *Cr species* | *Reference* | *Cr species* | *Reference* | *Cr species* | *Reference* |
| Cr | J6/73 | CrCl | BE95 | CrS(1) | IB77 |
| CrN | J12/73 | $CrCl_2$ | BE95 | CrS(2) | IB77 |
| CrO | J12/73 | CrOCl | BE95 | $Cr_2(SO_4)_3(s)$ | IB89 |
| CrOH | BE93 | $CrCl_3$ | BE95 | | |
| $CrO_2$ | J12/73 | $CrOCl_2$ | BE95 | | |
| CrOOH | BE93 | $CrCl_4$ | BE95 | | |
| $Cr(OH)_2$ | BE93 | $CrO_2Cl$ | BE95 | | |
| $CrO_3$ | J12/73 | $CrOCl_3$ | BE95 | | |
| $CrO_2OH$ | BE93 | $CrCl_5$ | BE95 | | |
| $Cr(OH)_3$ | BE93 | $CrO_2Cl_2$ | BE95 | | |
| $CrO(OH)_3$ | BE95 | $CrOCl_4$ | BE95 | | |
| $CrO(OH)_2$ | BE93 | $CrCl_6$ | BE95 | | |
| $CrO_2(OH)_2$ | BE93 | $CrCl_2(s)$ | IB89 | | |
| $Cr(OH)_4$ | BE93 | $CrCl_2(l)$ | IB89 | | |
| $CrO(OH)_4$ | BE93 | $CrCl_3(s)$ | IB89 | | |
| $Cr(OH)_5$ | BE93 | | | | |
| $Cr(OH)_6$ | BE93 | | | | |
| Cr(*s*) | J6/73 | | | | |
| Cr(*l*) | J6/73 | | | | |
| $Cr_7C_3(s)$ | IB89 | | | | |
| $Cr_3C_2(s)$ | IB93 | | | | |
| $Cr_{23}C_6(s)$ | IB89 | | | | |
| $Cr(CO)_6(s)$ | IB89 | | | | |
| CrN(*s*) | J12/73 | | | | |
| $Cr_2N(s)$ | J12/73 | | | | |
| $CrO_2(s)$ | IB89 | | | | |
| $CrO_3(s)$ | IB89 | | | | |
| $CrO_3(l)$ | IB89 | | | | |
| $Cr_2O_3(s)$ | J12/73 | | | | |
| $Cr_2O_3(l)$ | J12/73 | | | | |

J6/73: JANAF 6/73–Chase (1986); J12/73: JANAF 12/73–Chase (1986); J12/76: JANAF 12/76–Chase (1986); J3/77: JANAF 3/77–Chase (1986); J9/77: JANAF 9/77–Chase (1986); L2/84: Lewis 2/84–McBride *et al.* (1993); L3/84: Lewis 3/84–McBride *et al.* (1993); BE93–Ebbinghaus (1993); BE95–Ebbinghaus (1995); BAR73–Barin (1973); IB77–Barin (1977); IB89, B5/89–Barin (1989); IB93–Barin (1993).

TABLE II Nominal experimental mass feed rates

| *Fuel/oxidant species* | *Feed rate* | *g-moles/min* | |
|---|---|---|---|
| $CH_4$ | 86.09 L/min | 3.74 | |
| $O_2$ @ SR = 1.2 | 209.91 L/min | 8.75 | |
| $N_2$ @ SR = 1.2 | 789.67 L/min | 32.79 | |
| | *Feed rate* | *g-moles/min* | *Calculated stack ppm$_v$* |
| Cr(III) tests | | | |
| $Cr(NO_3)_3$(III) | 1.26 g/min | 0.0053 | 115 (Cr) |
| $H_2O$ | 17.11 g/min | 0.95 | – |
| $Cl_2$ | 0.61 L/min | 0.027 | 1180 (Cl) |
| | 1.52 L/min | 0.68 | 2930 (Cl) |
| $SO_2$ | 1.16 L/min | 0.052 | 1120 (S) |
| | 2.90 L/min | 0.13 | 2800 (S) |
| Cr(VI) tests | | | |
| $CrO_3$(IV) | 0.52 g/min | 0.0052 | 112 (Cr) |
| $H_2O$ | 17.27 g/min | 0.96 | – |
| $Cl_2$ | 0.61 L/min | 0.027 | 1180 (Cl) |
| | 1.52 L/min | 0.068 | 2930 (Cl) |
| $SO_2$ | 0.087 L/min | 0.0039 | 84 (S) |
| | 0.29 L/min | 0.013 | 280 (S) |
| | 1.16 L/min | 0.052 | 1120 (S) |
| | 2.90 L/min | 0.13 | 2800 (S) |
| Ni tests | | | |
| $Ni(NO_3)_2$ | 0.91 g/min | 0.0049 | 108 (Ni) |
| $H_2O$ | 17.50 g/min | 0.97 | – |
| $Cl_2$ | 0.52 L/min | 0.024 | 1000 (Cl) |

chlorine, high temperature sorbents might be able to capture Ni, but are less likely to capture Cr because (reactive) sorbent capture of a metal requires that metal to first be vaporized. Experimental work is required to test this hypothesis. At low temperatures ( < 500 K), Ni and chlorine are predicted to form a condensed Ni-chloride salt, thus rendering the residue water soluble. Chlorine's predicted effect on Cr at low temperatures ( < 600 K) is profound. Not only is Cr predicted to form vapor-phase Cr-chlorides, but it is also predicted to form the Cr(VI)-chlorides, $CrOCl_4$ and $CrCl_6$ (indicated on Fig. 1b).

The presence of sulfur (Fig. 1c) completely eliminates the chlorine enhanced formation of low temperature Cr(VI) species, but has little effect on the high temperature Cr(VI) species (not shown on Fig. 1, see Linak *et al.*, 1996). This is because sulfur ties up Cr to form Cr(III)-sulfate, but only at low temperatures. The effect of sulfur on the Ni/chlorine mixture is quite predictable. It has no effect at high temperatures on the devolatilization of Ni, since Ni-sulfates are unstable there, while its effect at low temperatures

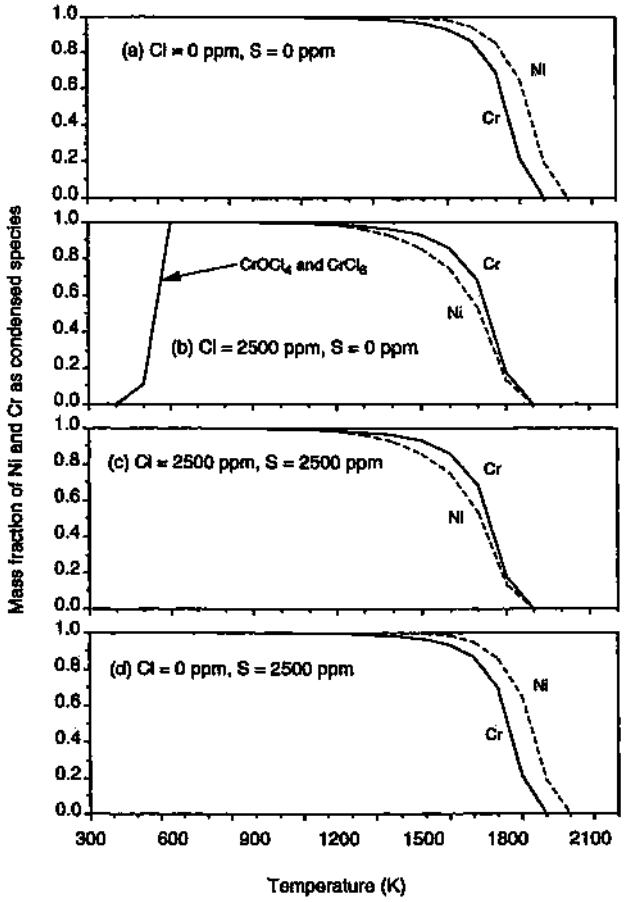


FIGURE 1 Ni and Cr equilibrium predictions for four experimental conditions: (a) 0 ppm chlorine, 0 ppm sulfur; (b) 2500 ppm chlorine, 0 ppm sulfur; (c) 2500 ppm chlorine, 2500 ppm sulfur; and (d) 0 ppm chlorine, 2500 ppm sulfur. Table I presents Ni and Cr species considered. Table II presents input concentrations used for fuel and oxidant species. Ni and Cr concentrations were 100 ppm. Lines represent total condensed species.

(< 900 K) is merely to replace a solid Ni-chloride by a solid Ni-sulfate. Additional calculations exploring the effects of calcium's affinity for sulfur showed that calcium, even at concentrations in excess with respect to sulfur, displaced neither the Ni- nor the Cr-sulfate and, therefore, had no appreciable effect on Ni or Cr partitioning.

The volatility behavior of Ni and Cr in the presence of sulfur only (Fig. 1d) is similar to their behavior without sulfur (Fig. 1a). At higher temperatures, Ni- and Cr-sulfates are not predicted to be stable, and at low

temperatures (< 900 K for Ni and < 800 K for Cr) solid phase Ni- and Cr-sulfates are predicted to replace solid phase Ni- and Cr-oxides.

## EXPERIMENTAL APPARATUS AND EXPERIMENTAL PROCEDURE

### Laboratory Swirl Flame Combustor

Experiments were performed using the laboratory scale 59 kW (actual), 82 kW (maximum rated) horizontal tunnel combustor presented in Figure 2. This refractory-lined research combustor was designed to simulate the time/temperature and mixing characteristics of practical industrial liquid and gas combustion systems. Natural gas fuel, aqueous metal solutions, gas dopants, and combustion air were introduced into the burner section through an International Flame Research Foundation (IFRF) moveable-block variable-air swirl burner. This burner incorporates an interchangeable injector positioned along its center axis. Swirling air passes through the annulus around the fuel injector promoting flame stability and attachment to the water-cooled quarl. A high swirl (IFRF Type 2) flame with internal

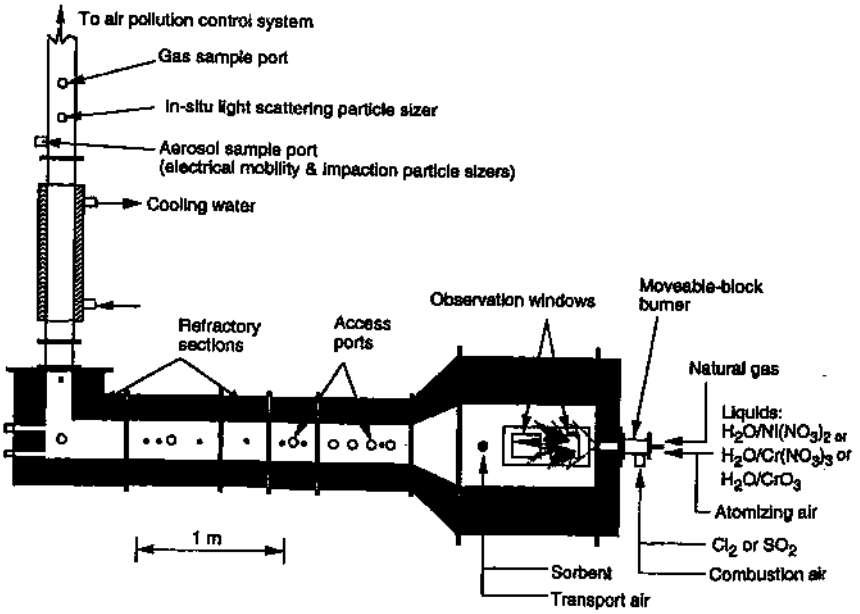


FIGURE 2 EPA horizontal tunnel combustor.

recirculation (Swirl No. = 1.48) was used. Gaseous and aerosol samples were taken from a stack location 5.9 m from the burner quarl. The temperature at this location was approximately 670 K (745°F). Figure 2 also indicates where sorbents were injected for those few experiments where sorbents were examined. The method of injection and the composition and surface characteristics of the kaolinite and hydrated lime sorbents are described by Linak *et al.* (1995). The temperature profile for the standard 59 kW experiments (without oxygen enrichment) has been published previously (Linak *et al.*, 1994). Further details regarding the experimental combustor can be found elsewhere (Linak *et al.*, 1994, 1995, 1996).

## Metal Systems Investigated

Ni-nitrate [$Ni(NO_3)_2$], Cr(III)-nitrate [$Cr(NO_3)_3$], or Cr(VI)-oxide [$CrO_3$] were introduced as aqueous solutions through a special fuel/waste injector which incorporated a small air atomizing system down the center of a standard natural gas injector. The resulting droplet PSD was relatively narrow with a mean droplet diameter of approximately 50–80 μm (Linak *et al.*, 1994). Diatomic chlorine ($Cl_2$) or sulfur dioxide ($SO_2$) dopants were introduced, separately from the metal solutions, with the (secondary) combustion air. Thus, the metal, chlorine, or sulfur, were not mixed prior to their introduction into the combustor. All interactions between the components were dependent upon normal turbulent mixing patterns.

Aqueous solutions containing 1.5% (by weight) Ni and Cr were used. Solution flow rates were maintained so as to produce stack gas concentrations of approximately 100 ppm metal (by volume). Metal feed rates presented in Table II correspond to constant molar feed rates of approximately 0.005 g-moles/min. Several tests were performed to introduce $Cl_2$ or $SO_2$ at different molar ratios of chlorine or sulfur to metal. These feed rates and resulting stack concentrations (calculated) are also presented in Table II. Excess air was maintained at 20%. No air preheat was employed.

## Chromium Speciation: Sampling and Analysis

In contrast to Ni, analytical measurement of total Cr and Cr(VI) is particularly difficult because the likely dominant Cr species [$Cr_2O_3(s)$] is extremely difficult to digest for subsequent analysis and care must be taken to ensure that Cr(VI) is not reduced during the sampling and analysis process. Cr(VI) is stabilized by keeping the sample in contact with an alkaline environment at all times. The converse problem of Cr oxidation to

Cr(VI) species is not an issue at room temperatures (Seigneur and Constantinou, 1995).

Samples were analyzed for both Cr(VI) and total Cr. Cr(VI) analyses were performed using ion chromatography with a post-column reactor (IC/PCR) and a visible wavelength detector, as described in the Methods Manual for Compliance with the BIF Regulations, EPA Method 0061 (Garg, 1990a). These same samples were also analyzed for total Cr by a caustic fusion procedure. In this method, the sample filtrate was placed in a graphite crucible and "fused" with 1 g of sodium nitrate ($NaNO_3$) and 3 g of sodium hydroxide (NaOH) in a muffle furnace. During fusion, the crucible and contents were heated over a 4 hour period from 250°C to 410°C with 1 hour stops at 350 and 390°C. Upon cooling, the sample was dissolved in approximately 60 mL of deionized water over a hot plate and then diluted to 100 mL in a volumetric flask with 2 mL of concentrated nitric acid ($HNO_3$) added. The digested samples were analyzed by graphite furnace atomic absorption (GFAA). This method produced notably improved digestion efficiencies (75%, 87% and 91%) compared to the hydrofluoric acid (HF) digestion efficiencies (44% and 72%) outlined in the EPA Method 0060 (Garg, 1990b) procedures. Further discussion of these analytical methods are presented by Linak *et al.* (1996).

## Aerosol Particle Size Distribution: Sampling and Analysis

PSD measurements were taken from the stack location using three techniques. Extractive samples were taken for collection by inertial impaction and electrical mobility analyses using an isokinetic aerosol sampling system based on the modified designs of Scotto *et al.* (1992) and Linak *et al.* (1994). In order to minimize in-probe gas and aerosol kinetics, the sampling system dilutes and cools the aerosol sample using filtered nitrogen and air immediately after sampling. Dilution ratios are measured directly for each experiment and verified independently by the measurement of a nitric oxide tracer gas.

Extracted samples were directed to an Andersen Inc. eight stage, 28.3 L/min. (1 $ft^3$/min.), atmospheric pressure cascade impactor and a Thermo-Systems Inc. scanning mobility particle sizer (SMPS). The cascade impactor is designed to collect physical samples (for subsequent gravimetric and/or chemical analysis) on nine stages (including the after filter) less than approximately 10 μm diameter. The SMPS classifies and counts particles within a working range of 0.01 to 1.0 μm diameter using principles of charged particle mobility through an electric field. The SMPS, used

throughout the Cr experiments, is an upgraded version of the differential mobility particle sizer (DMPS), used during the Ni experiments. The SMPS upgrade allows for improved PSD resolution and shorter sampling times. The SMPS and DMPS were configured to yield 54 and 27 channels, respectively, evenly spaced (logarithmically) over the 0.01 to 1.0 μm diameter range.

In addition to the inertial impaction and electrical mobility devices which require an extracted sample, limited *in-situ* light scattering PSDs were taken using an Insitec Inc. laser doppler velocimeter. This instrument determines particle size by measuring the light scattering intensity of particles which pass through a sampling volume established within the combustor stack by a laser focused through a set of quartz optical access ports. This instrument was available for only several Cr experiments and was not available at all during the Ni experiments. The working range of this device was approximately 0.3 to 30 μm diameter which slightly overlapped and extended the PSD data collected by the SMPS.

In addition to the three PSD instruments, samples were collected on silver filters and analyzed using a field emission scanning electron microscope (SEM) equipped with an energy dispersive X-ray (EDX) spectrometer. This provided morphological information as well as qualitative chemical analysis of individual particles.

## RESULTS AND DISCUSSION

### Particle Size Distributions without Chlorine

Figure 3 presents the PSDs for Ni [injected as $Ni(NO_3)_2$], for Cr(III) [injected as $Cr(NO_3)_3$], and for Cr(VI) [injected as $CrO_3$]. As described above, these aqueous solutions were injected through a natural gas diffusion flame operated at 20% excess oxygen ($SR = 1.2$). These data (open symbols) were obtained using the SMPS for particles in the 0.01 to 1.0 μm diameter size range and the *in-situ* light scattering particle sizer for particles in the 0.3 to > 10 μm diameter size range. Each panel also shows the effect of chlorine addition (solid symbols), where the chlorine was added as $Cl_2$ gas, with the secondary combustion air. Figure 4 shows the results of gravimetric analyses of masses collected on the eight stages and after filter of the cascade impactor. The mass fraction of the metal collected is plotted *versus* particle diameter. The particle diameter, denoted by the abscissa value at left side of each bar, is that particle diameter at which 50% of the particles fail to be

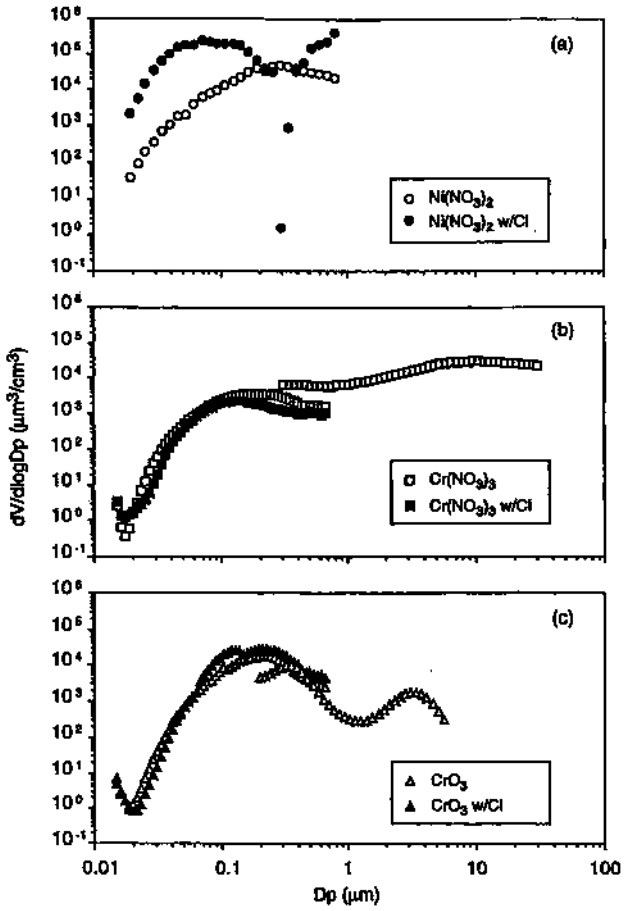


FIGURE 3 Particle volume distributions measured by electrical mobility and light scattering for: (a) $Ni(NO_3)_2$; (b) $Cr(NO_3)_3$; and (c) $CrO_3$ aqueous solution feeds with and without chlorine. Chlorine concentrations were 1000 and 2900 ppm for the Ni and Cr experiments, respectively.

collected by the impactor plate in question (50% cutoff diameter). All particle sizes in Figure 4 have been corrected for particle density effects.

It should be noted that all three methods of particle collection and sizing produced consistent results. Data from the *in-situ* light scattering particle sizer slightly overlapped and extended the range of the SMPS for the sampled particles. This suggests that the isokinetic dilution sampling procedure used maintained aerosol size integrity.

The Ni SMPS volume PSD without chlorine (Fig. 3a) showed a maximum at about 0.3–0.4 μm diameter, and this is corroborated by the correspond-

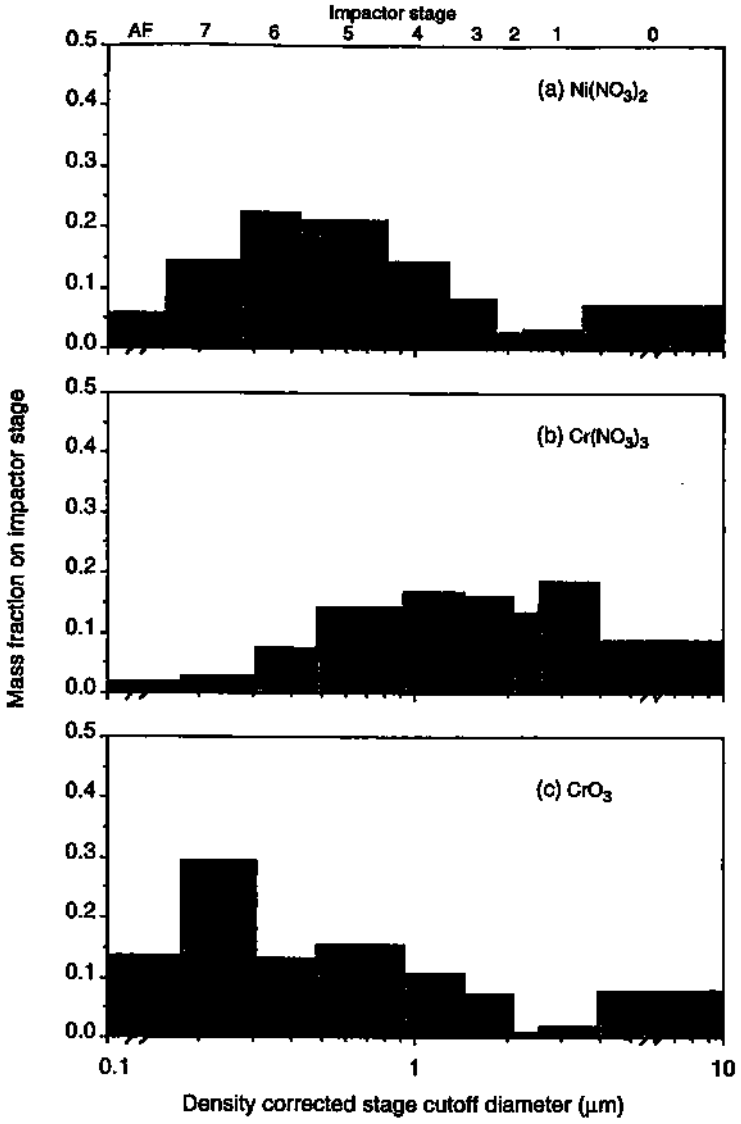


FIGURE 4 Particle mass fraction distributions measured by gravimetric inertial impaction for: (a) $Ni(NO_3)_2$; (b) $Cr(NO_3)_3$; and (c) $CrO_3$ aqueous solution feeds. No chlorine added.

ing impactor results on Figure 4a. These diameters are somewhat smaller than the 2 μm mean diameter that was calculated for the residual Ni particles remaining after the liquid solvent vaporized. This suggests that some form of fragmentation occurred. For Cr(III) without chlorine, a single

particle size mode peaking between 1.0 and 10 μm diameter is shown by both the *in-situ* light scattering particle sizer data (Fig. 3b) and the impactor data (Fig. 4b). For Cr(VI), two modes are apparent from the SMPS and the *in-situ* light scattering particle sizer, with a dominant mode peaking at about 0.1–0.3 μm diameter (Fig. 3c). This is verified by the impactor results (Fig. 4c), which also show a dominant mode at about 0.2–0.3 μm diameter. These results suggest that $CrO_3$ vaporized, while $Cr(NO_3)_3$ did not. The difference in volatilization behavior of the two Cr compounds is, of course, in contrast to equilibrium predictions, which are independent of the initial Cr speciation. Because there was some doubt that these small particles were caused by vaporization, additional experiments were conducted to investigate whether one could create additional volatilization (as demonstrated by the appearance of larger amounts of even smaller fume particles) by imposing substantially higher combustion temperatures. Figure 5 presents additional data for $CrO_3$ resulting from higher temperature experiments, where oxygen enrichment (24–26%) produced measured temperatures that were approximately 125 K higher. Figure 5 depicts no significant change in the Cr PSD and no evidence of additional vaporization, most probably because the $CrO_3$ was extensively vaporized under all conditions examined. Under baseline conditions, the particles were collected primarily on the bottom impactor plate (stage 7) (see Fig. 4c), rather than on the after filter, because the high Cr dewpoint still allowed substantial particle coagulation to occur before sampling. Due to instrument availability, the coarse mode was not measured for the experiments described on Figure 5. This was also the case for a portion of the data presented in Figures 3b, c.

## Effect of Chlorine

Chlorine has a significant effect on the number and volume PSDs for Ni. The maximum number concentration now occurs at 0.03 μm diameter (data not shown), while the maximum volume concentration has shifted to particle diameters less than 0.1 μm (Fig. 3a). These PSDs are consistent with a nucleation/vaporization mechanism for Ni in the presence of chlorine. The Cr results, by contrast, show no effect on the stack PSD by chlorine, as illustrated by comparison of open and solid symbols on Figures 3b, c. In the case of $Cr(NO_3)_3$, the chlorine did not facilitate vaporization, while in the case of $CrO_3$, which vaporized without chlorine, no difference in PSD was noted. Thus, the PSDs from neither $Cr(NO_3)_3$ nor $CrO_3$ were affected by chlorine. With oxygen enrichment (Fig. 5) chlorine appeared to produce a

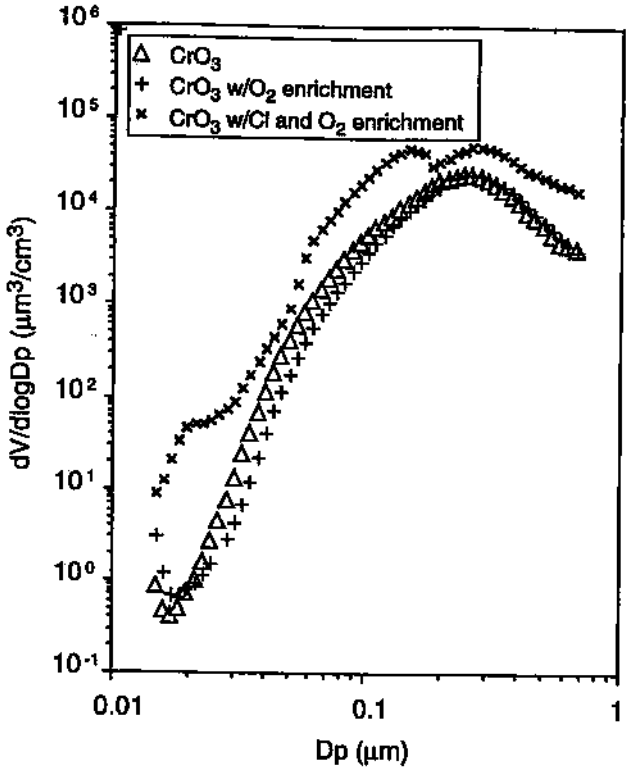


FIGURE 5 Particle volume distributions measured by electrical mobility for $CrO_3$ aqueous solution feeds with oxygen enrichment of the combustion air (24–26% $O_2$) and with oxygen enrichment and chlorine.

slight increase in the number of small particles, and also produced a multi-modal PSD, possibly because of the appearance of multiple chlorinated Cr species with different nucleation characteristics. This multi-modal behavior is also evident for $CrO_3$ without oxygen enrichment (Fig. 3c) and is not predicted by equilibrium (Linak *et al.*, 1996). However, comparisons between the Ni and Cr results are qualitatively consistent with the equilibrium predictions of Figure 1, which show the effect of chlorine to be that of moving the Ni dewpoint from above that of Cr to below that of Cr. According to both theory and experiment, chlorine facilitates Ni volatilization at high temperatures, but has little effect on Cr. Note, however, that results are inconsistent with the low temperature equilibrium predictions of Cr with chlorine, since the Cr was found to condense at low temperature [*i.e.*, the predicted equilibrium yield of almost 100% of the Cr(VI) compounds, gaseous $CrOCl_4$ and $CrCl_6$, was not observed].

## Scanning Electron Micrographs

In the absence of chlorine, neither $Ni(NO_3)_2$ nor $Cr(NO_3)_3$ appeared to vaporize, although $CrO_3$ did. Yet, even in the absence of vaporization, a significant quantity of submicron particles were formed (Figs. 3 and 4). The issue now is to explain how small particles are created from refractory compounds, without having recourse to vaporization/nucleation processes. Mulholland and Sarofim (1991) and Mulholland *et al.* (1991) have shown that $Ni(NO_3)_2$ can form cenosopheres, which can fragment to form small particles. In their studies, this yielded a tri-modal PSD (using a cascade impactor). This tri-modal behavior was not observed here with either the impactor or the SMPS. Differences in heating rates in the two experiments are thought to account for this. Although no cenospheres with single blow-holes were observed in samples taken from these experiments, the possibility of fine particle formation through other fragmentation mechanisms is quite possible.

Figure 6 presents a series of three magnifications of a secondary electron image of an exhaust particulate sample from the $Cr(NO_3)_3$ experiments with chlorine present. Figure 6a (3000 X magnification) shows a coagulated agglomerate on a silver filter. Figure 6b (9000 X) shows greater detail and suggests that a variety of particle shapes are present. Figure 6c (45000 X) distinctly shows the presence of tiny, well formed crystals, with angular sides. EDX analyses show that the elongated crystal located in the right center (Fig. 6c) contains Cr but no chlorine, while the fused sphere in the upper left corner (Fig. 6c) contains both Cr and chlorine. The mechanism by which the tiny crystals were formed, and by which chlorine is found within only a limited number of spherical particles is not known. Sintering mechanisms may come into play. Secondary electron images of the samples from the $CrO_3$ experiments show a very finely divided amorphous powder, and were very different from those shown on Figure 6. These results support the hypothesis that the two Cr species followed very different mechanistic paths from inlet to sample. However, based on sample color and poor acid solubility, the predominant Cr species sampled for all the Cr experiments is believed to be $Cr_2O_3$[Cr(III)], which is the predicted predominant stable Cr species between 900 and 1400 K (Linak *et al.*, 1996). This was independent of whether $Cr(NO_3)_3$ or $CrO_3$ was fed.

## Cr Partitioning

Although the primary focus of this paper is on factors influencing PSDs, chemical speciation is also of paramount importance, as far as Cr is

concerned. Equilibrium predictions of Cr speciation (Linak *et al.*, 1996) suggested that in the absence of chlorine, the fraction of Cr(VI) is small and appears only at the higher temperatures. When chlorine is added, two additional Cr(VI) species are predicted to appear at lower temperatures [$CrOCl_4$ and $CrCl_6$]. EDX analysis (Fig. 6) shows that chlorine is found only

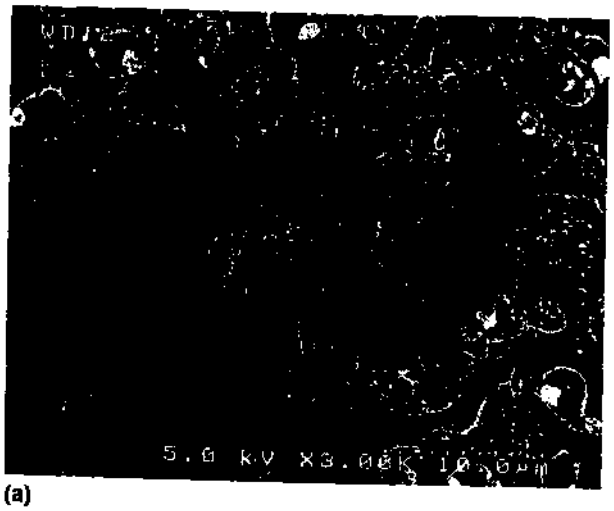


(a)


(b)

FIGURE 6 Field emission scanning electron micrographs of particles collected on a silver filter during $Cr(NO_3)_3$ aqueous solution feeds with chlorine: (a) 3,000 X; (b) 9,000 X; and (c) 45,000 X.

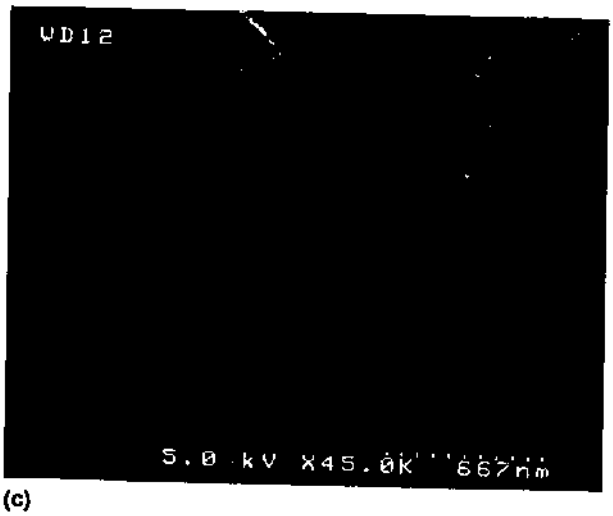


(c)

FIGURE 6 (Continued).

on the fused spherical particles, and not on the angular crystalline particles. One might speculate that the fused particle may contain Cr including the Cr(VI) compounds, $CrOCl_4$ and/or $CrCl_6$. However, since the equilibrium calculations at low temperatures fail to predict the existence of a solid species containing Cr, one might conclude that kinetic limitations prevent significant Cr(VI) formation. Whatever the formation route to chlorinated Cr in the exhaust, sulfur is predicted by equilibrium (Fig. 1d) to eliminate those species and, thus, (potentially) eliminate one source of Cr(VI).

Shaded symbols on Figure 7 denote the fraction of measured Cr that appeared as Cr(VI) in the stack as a function of the stack sulfur concentration. Chlorine has been shown to enhance Cr(VI) formation (Linak *et al.*, 1996). As shown in Figure 7, less than 1% of the total Cr was measured as Cr(VI). This is a slightly smaller percentage than presented by Linak *et al.* (1996). However, that study examined higher chlorine concentrations ( > 6000 ppm). As sulfur is added, the fraction of Cr(VI) decreases to below analytical detection limits. The sensitivity of Cr speciation to sulfur addition is notable. Less than 100 ppm $SO_2$ addition (2900 ppm chlorine) decreased the Cr(VI) fraction to below analytical detection limits. This is qualitatively consistent with equilibrium predictions (shown as lines on Fig. 7), where speciation data are compared to equilibria at two different temperatures. Equilibrium predictions of Cr(VI) are extremely sensitive to temperature (see Linak *et al.*, 1996). However, no particular significance should be placed on these temperatures since they

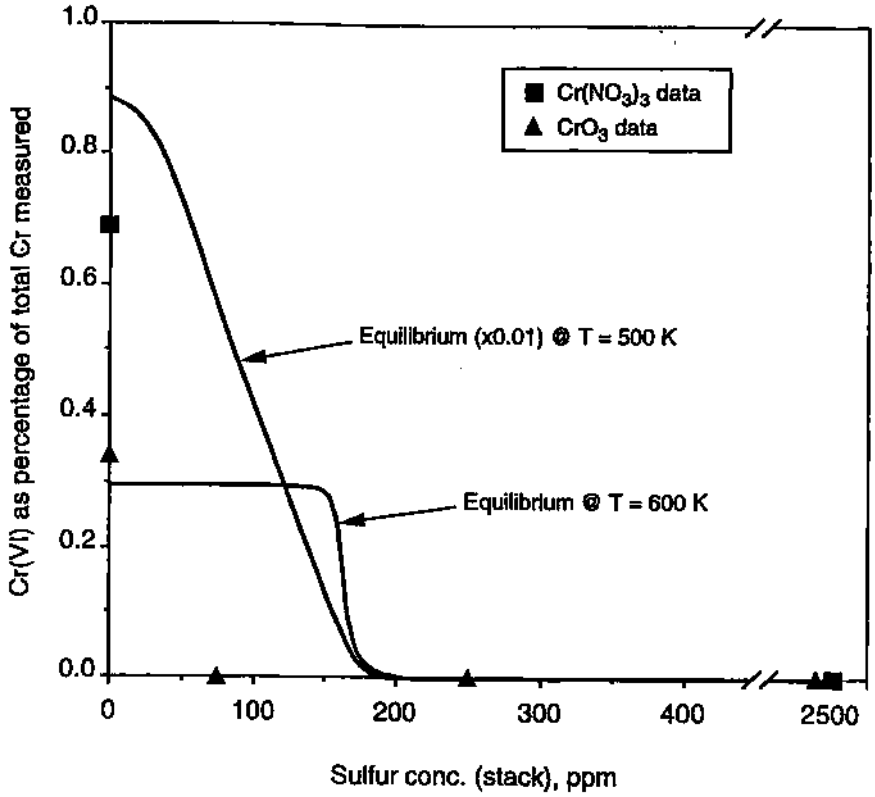


FIGURE 7 Effect of sulfur (stack) concentration on Cr(VI) emissions. Shaded symbols represent experimental data for $Cr(NO_3)_3$ and $CrO_3$ aqueous solution feeds. Lines represent equilibrium predictions at 500 K and 600 K. Cr and chlorine concentrations were 100 and 2900 ppm, respectively.

were chosen arbitrarily, with $T = 600$ K shown only because it allowed Cr partitioning to be matched for the 0 ppm sulfur case. Both theory and experiment suggest that sulfur is so effective in eliminating Cr(VI) because it displaces chlorine from the Cr(VI) compounds otherwise formed without sulfur. Both theory and experiment suggest that only a very small amount of sulfur, determined by the Cr/sulfur stoichiometry, is sufficient to suppress formation of chlorinated Cr(VI) compounds.

## Sorbent Scavenging of Refractory Metals

One would not expect metals that are not vaporized to be scavenged by sorbents, such as kaolinite or lime. Since vaporization of both $Ni(NO_3)_2$

(with chlorine) and $CrO_3$ (with and without chlorine) was noted to have occurred, it is appropriate to investigate metal/sorbent interactions for all the cases reported on Figure 3.

The results for Ni are especially interesting. Ni without chlorine does not vaporize (Figs. 3a and 4a) and, therefore, cannot react as a vapor with kaolinite sorbent (Fig. 8a). Note how the effect of kaolinite addition is only to add to the coarse particle size mode (at 1.0 μm diameter, which is at the

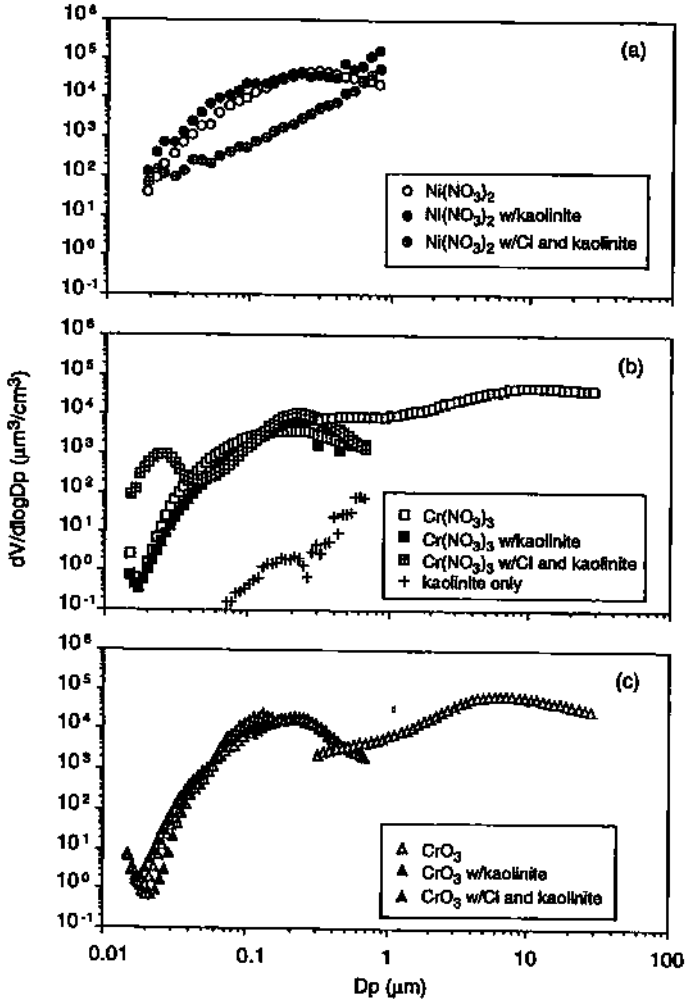


FIGURE 8 Particle volume distributions measured by electrical mobility and light scattering for: (a) $Ni(NO_3)_2$; (b) $Cr(NO_3)_3$; and (c) $CrO_3$ aqueous solution feeds with and without kaolinite and chlorine.

upper limit of the SMPS data), and the smaller particles are not affected. This is consistent with coagulation theory (Linak and Wendt, 1993) which indicates that coagulation between small and large particles is too slow to enable metal particle scavenging by sorbent particles. When chlorine is added, Ni appears to vaporize (Fig. 3a) and, consequently, it also appears to interact with kaolinite, as shown by the decrease in the very small particle mode which was present without the sorbent (Fig. 8a). Hence, chlorine allows Ni to volatilize and consequently be scavenged by kaolinite. The pertinent mechanism may, however, be quite complicated, since other research (Scotto *et al.*, 1992 and Linak *et al.*, 1995) has shown that chlorine tends to diminish the reaction rate for the scavenging of cadmium and lead by kaolinite. These two conflicting effects must be accounted for.

Figure 8 also shows the effects, or rather the lack of an effect, of kaolinite injection on the Cr PSD for both $Cr(NO_3)_3$ and $CrO_3$. For $Cr(NO_3)_3$, this is not surprising, since that compound did not vaporize. However, there was also no sorbent scavenging effect on $CrO_3$, even though that compound was believed to vaporize. Possible explanations include low interaction affinity between Cr and kaolinite and the possibility that the Cr vapor may not have been present long enough to contact the sorbent, which was injected downstream of the flame (see Fig. 2). Figures 3 and 4 show that Cr from $CrO_3$ underwent coagulation over a longer period of time than did Ni with chlorine, presumably because it had a higher effective dewpoint. Lime also had a negligible effect on the PSDs from $Cr(NO_3)_3$ and $CrO_3$, and so it can be concluded that lime is an ineffective sorbent for all forms of Cr tested, whether vaporization occurred or not.

## CONCLUSIONS

Three methods for measuring PSDs in combustor exhausts yielded consistent results. The extractive sampling methods followed by electrical mobility analysis and inertial impaction agreed well with *in-situ* stack analyses using light scattering. Ni did not vaporize under baseline conditions, but did vaporize upon the introduction of chlorine (with the combustion air). When it vaporized, a portion of the Ni (70–80%) could be scavenged by kaolinite.

Whether Cr vaporized depended on the form in which Cr entered the combustor. When it was introduced as aqueous $Cr(NO_3)_3$ [Cr(III)] it did not vaporize, even upon the addition of chlorine. When it was introduced as aqueous $CrO_3$ [Cr(VI)], it did vaporize, both with or without chlorine

present. No matter how in entered, or whether, indeed, it vaporized, Cr in the exhaust contained very little Cr(VI). The mechanistic paths which Cr follows upon its introduction into a furnace are not known, but depend on the initial form of the metal, even though the ultimate speciation does not. Submicron metal crystals were observed for Cr that did not vaporize, suggesting that physical as well as chemical processes play important roles in determining resultant PSDs. Chlorine enhanced Cr(VI) formation in the exhaust. However, even in the presence of 2900 ppm chlorine, a maximum of less than 1% of the total Cr measured in the exhaust was Cr(VI). This fraction of Cr(VI) could be reduced below analytical detection limits by stoichiometric (with respect to Cr) addition of sulfur.

In general, equilibrium predictions were useful in explaining the experimental data. This was especially true for the effects of sulfur on Cr(VI). Equilibria could not predict the observed effects of inlet Cr speciation, but were useful in explaining how chlorine influenced Ni vaporization without having a significant effect on Cr. Quantitative predictions from equilibria, however, should be made with due caution.

## Acknowledgements

Portions of this work were conducted under EPA Purchase Orders 4D2910NATX and 5D2727NATX with J. O. L. Wendt and EPA Contract 68-D4-0005 with Acurex Environmental Corp. The authors gratefully acknowledge the contributions of C. Elmore, P. Groff, and D. Janek of Acurex Environmental Corp., to the experimental efforts as well as the contribution of K. Luk of Research Triangle Institute, for the caustic fusion digestion procedure. The research described in this article has been reviewed by the Air Pollution Prevention and Control Division, U.S. Environmental Protection Agency, and approved for publication. The contents of this article should not be construed to represent Agency policy nor does mention of trade names or commercial products constitute endorsement or recommendation for use.

## References

Barin, I., Knacke, O. and Kubaschewski, O. (1977) Thermochemical properties of inorganic substances, supplement, Springer-Verlag, New York, NY.

Barin, I. (1989) Thermochemical data of pure substances, VCH Verlagsgesellschaft, New York, NY.

Barin, I., Knacke, O. and Kubaschewski, O. (1973) Thermochemical properties of inorganic substances, Springer-Verlag, New York, NY.

Barin, I. (1993) Thermochemical data of pure substances, VCH Verlagsgesellschaft, New York, NY.

CAAA-Clean Air Act Amendments (1990) Public Law 101–549, 104 Stat. 2399–2712, November 15.

Chase, M. W. Jr. (1986) JANAF Thermochemical tables, 3rd edn., parts 1 and 2, American Institute of Physics, New York, NY.

Clarke, L. B. and Sloss, L. L. (1992) Trace elements–emissions from coal combustion and gasification, IEA Coal Research, IEACR/49, London.

Davison, R. L., Natusch, D. F. S., Wallace, J. R. and Evans, C. A. Jr. (1974) Trace elements in fly ash dependence of concentration on particle size, *Environ. Sci. Technol.*, **8**(13), 1107–1113.

Ebbinghaus, B. B. (1993) Thermodynamics of gas phase chromium species: the chromium chlorides, oxychlorides, fluorides, oxyfluorides, hydroxides, oxyhydroxides, mixed oxyfluorochlorohydroxides, and volatility calculations in waste incineration processes, *Combust. and Flame*, **101**, 119–137.

Ebbinghaus, B. B. (1995) Thermodynamics of gas phase chromium species: the chromium oxides, chromium oxyhydroxides, and volatility calculations in waste incineration processes, *Combust. and Flame*, **93**, 311–338.

Federal Register, (1991) Vol. 56, no. 35, February 21, 1991, U.S. EPA Office of Solid Waste, Guidance on metal and hydrogen chloride controls for hazardous waste incinerators, volume IV of the hazardous waste incineration guidance series, Hazardous waste: boilers and industrial furnaces; burning of hazardous wastes, 7134, Washington, DC.

Frandsen, F., Dam-Johansen, K. and Rasmussen, P. (1994) Trace elements from combustion and gasification of coal – an equilibrium approach, *Prog. Energy Combust. Sci.*, **20**, 115–138.

Garg, S. (1990a) EPA Method 0060 – Methodology for the determination of metals emissions in exhaust gases from hazardous waste incineration and similar combustion processes, in Methods Manual for Compliance with the BIF Regulations: Burning Hazardous Waste in Boilers and Industrial Furnaces, EPA/530-SW-91-010 (NTIS PB91-120006), pp. 3–1 through 3–48, Washington, DC.

Garg, S. (1990b) EPA Method 0061 – Determination of hexavalent chromium emissions from stationary sources, in Methods Manual for Compliance with the BIF Regulations: Burning Hazardous Waste in Boilers and Industrial Furnaces, EPA/530-SW-91-010 (NTIS PB91-120006), pp. 3–49 through 3–69, Washington, DC.

Garg, S. (1992) Technical Implementation Document for EPA's Boiler and Industrial Furnace Regulations, EPA-530/R-92-011 (NITS PB92-154947), U.S. EPA, Office of Solid Waste, Washington, DC.

Gordon, S. and McBride, B. J. (1986) Computer program for calculation of complex chemical equilibrium compositions, rocket performance, incident and reflected shocks, and Chapman-Jouguet detonations, NASA SP-273, Interim Revision.

Goyer, R. A. (1991) Toxic effects of metals, in Casarett and Doull's toxicology the basic science of poisons, 4th edn., Amdur, M. O., Doul, J. and Klaassen, C. D., Eds., Pergamon Press, New York, NY.

Klein, D. H., Andren, A. W., Carter, J. A., Emery, J. F., Feldman, C., Fulkerson, W., Lyon, W. S., Ogle, J. C ., Talmi, Y., VanHook, R. I. and Bolton, N. (1975) Pathways of thirty-seven trace elements through coal-fired power plant, *Environ. Sci. Technol.*, **9**(10), 973–979.

Linak, W. P. and Wendt, J. O. L. (1993) Toxic metal emissions from incineration: mechanisms and control, *Prog. Energy Combust. Sci.*, **19**, 145–185.

Linak, W. P., Srivastava, R. K. and Wendt, J. O. L. (1994) Metal aerosol formation in a laboratory swirl flame incinerator, *Combust. Sci. Technol.*, **101**(1–6), 7–27.

Linak, W. P., Srivastava, R. K. and Wendt, J. O. L. (1995) Sorbent capture of nickel, lead, and cadmium in a laboratory swirl flame incinerator, *Combust. and Flame*, **100**, 241–248.

Linak, W. P., Ryan, J. V. and Wendt, J. O. L. (1996) Formation and destruction of hexavalent chromium in a laboratory swirl flame incinerator, *Combust. Sci. Technol.*, **116–117**, 479–498.

Markowski, G. R., Ensor, D. S., Hooper, R. G. and Carr, R. C. (1980) A submicron aerosol mode in flue gas from a pulverized coal utility boiler, *Environ. Sci. Technol.*, **14**(11), 1400–1402.

McBride, B. J., Gordon, S. and Reno, M. A. (1993) Coefficients for calculating thermodynamic and transport properties of individual species, NASA Technical Memorandum 4513.

Mulholland, J. A. and Sarofim, A. F. (1991) Mechanisms of inorganic particle formation during suspension heating of simulated aqueous wastes, *Environ. Sci. Technol.*, **25**(2), 268–274.

Mulholland, J. A., Sarofim, A. F. and Yue, G. (1991) The formation of inorganic particles during suspension heating of simulated wastes, *Environ. Prog.*, **10**(2), 83–88.

Owens, T., Wu, C. Y. and Biswas, P. (1995) An equilibrium analysis for reaction of metal compounds with sorbents in high temperature systems, *Chem. Eng. Comm.*, **133**, 31–52.

Quann, R. J. and Sarofim, A. F. (1982) Vaporization of refractory oxides during pulverized coal combustion, *19th Comb. (Int.) Symp.*, pp. 1429–1440, Comb. Inst., Pittsburgh.

RCRA-Resource conservation and recovery act (1986) Subtitle C, Sections 3001–3013, 42 N.S.C., Sections 6921–6934 (1976) and Supplement IV (1980) amended.

Rizeq, R. G., Hansell, D. W. and Seeker, W. R. (1994) Prediction of metals emissions and partitioning in coal-fired combustion systems, *Fuel Processing Technol.*, **39**, 219–236.

Scotto, M. A., Peterson, T. W. and Wendt, J. O. L. (1992) Hazardous waste incineration: the *in-situ* capture of lead by sorbents in a laboratory down-flow combustor, *24th Comb. (Int.) Symp.*, pp. 1109–1118, Comb. Inst., Pittsburgh.

Seigneur, C. and Constantinou, E. (1995) Chemical kinetic mechanism for atmospheric chromium, *Environ. Sci. Technol.*, **29**, 222–231.

Wendt, J. O. L. (1994) Combustion science for incineration technology, *25th Comb. (Int.) Symp.*, pp. 277–289, Comb. Inst., Pittsburgh.

Wu, C. Y. and Biswas, P. (1993) An equilibrium analysis to determine the speciation of metals in an incinerator, *Combust. and Flame*, **93**, 31–40.